Available online at www.sciencedirect.com
ScienceDirect
Thermochimica Acta 451 (2006) 174–180
thermochimica acta
www.elsevier.com/locate/tca

Interaction of benzoic acid, aspirin and *para*-hydroxy benzoic acid with dipalmitoyl phosphatidic acid vesicles

Lata Panicker *

Solid State Physics Division, Bhabha Atomic Research Centre, Mumbai 400085, India

Received 31 March 2006; received in revised form 29 September 2006; accepted 4 October 2006
Available online 13 October 2006

Abstract

The effect of benzoic acid (BA), aspirin (ASA) and *para*-hydroxy benzoic acid (*p*-HOBA) on the thermotropic behaviour and molecular mobility of dipalmitoyl phosphatidic acid (DPPA) vesicles has been investigated using DSC and ^{1}H NMR. These investigations were carried out with DPPA dispersion in both multilamellar vesicular (MLV) and unilamellar vesicular (ULV) forms. The DSC data indicated that the mechanism by which BA, ASA and *p*-HOBA interact with the DPPA is similar in MLV and ULV. In the presence of BA, ASA and *p*-HOBA, the gel to liquid crystal phase transition temperature (T_m) of the DPPA vesicles increases. The DPPA vesicles thus becomes more rigid in the presence of BA, ASA and *p*-HOBA molecules, due to increased interaction between the lipid headgroups. The increase in rigidity of the DPPA membrane was found to be maximum when doped with ASA and least when doped with salicylic acid (SA). There seems to be good correlation between the acidity of –COOH group present in the drugs and the increase in T_m value (representing rigidity). The transition width (Δ_m) decreases with increasing concentration of BA, ASA and *p*-HOBA, implying an enhanced co-operativity of the acyl chain. DSC and NMR data indicate that BA, ASA and *p*-HOBA molecules, at all concentrations are located close to the interfacial region of the DPPA bilayer but not in the acyl chain region.

Keywords: DPPA; DSC; NMR; Aspirin; Benzoic acid; *para*-Hydroxy benzoic acid

1. Introduction

Phosphatidic acid (PA) is an anionic phospholipids found in bacterial cell membranes [1]. PA is also present in the metabolic pathway of the synthesis of a few membrane phospholipids [2]. Despite the low concentration of PA in the biomembranes, its importance is due to the fact that it is responsible for a net negative charge on the surface of cell membrane [3]. Hence, it is of interest to investigate the mode of action of drugs in dipalmitoyl phosphatidic acid (DPPA) (Fig. 1a) liposomes [4–8]. DPPA bears two ionizable groups with pK_a values 3.9 and 8.6 [9], hence the negative surface charge of this membrane can be varied and the chain melting transition temperature, T_m, is pH-dependent [10].

Studies of DPPA vesicles containing salicylic acid (SA) (Fig. 1b) had shown that (a) the drug molecules are located in the neighborhood of the DPPA headgroup and (b) the drug interacts with DPPA vesicles by affecting both their thermotropic behaviour and their molecular mobility [11]. These results suggest that SA, besides its action on enzyme cyclooxygenase, could exert some of its effects through its interaction with the lipids of the membrane bilayer. In order to observe whether other aromatic compounds interact with DPPA vesicles, in a similar way, studies were carried out with benzoic acid (BA), aspirin (ASA) and *para*-hydroxy benzoic acid (*p*-HOBA) (Fig. 1c–e) doped DPPA systems. The aromatic compounds, SA, ASA, BA and *p*-HOBA have carboxylic acid (–COOH) as one of the functional groups with pK_a values 2.98, 3.5, 4.2 and 4.58, respectively. Thus the –COOH group in SA is the most acidic while the –COOH group in *p*-HOBA is the least acidic (the acidic strength, *S*, of –COOH group in these drugs are as follows: $S_{SA} > S_{ASA} > S_{BA} > S_{p\text{-HOBA}}$).

The non-steroidal anti-inflammatory drugs like SA and ASA are inhibitor of enzymes cyclooxygenase 1 (COX-1) and cyclooxygenase 2 (COX-2) which are responsible for

Abbreviations: DSC, differential scanning calorimetric; BA, benzoic acid; ASA, aspirin; *p*-HOBA, *para*-hydroxy benzoic acid; DPPA, dipalmitoyl phosphatidic acid; CM, chain melting; NMR, nuclear magnetic resonance

* Tel.: +91 22 25594075; fax: +91 22 25505151.
E-mail addresses: Lata_Panicker@yahoo.com, lata@magnum.barc.ernet.in.

0040-6031/$ – see front matter © 2006 Elsevier B.V. All rights reserved.
doi:10.1016/j.tca.2006.10.003

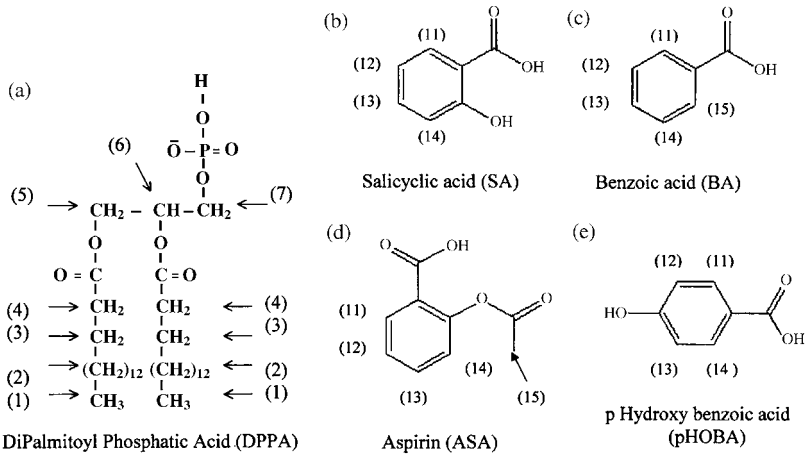

Fig. 1. Schematic structure of (a) the phospholipid, dipalmitoyl phosphatidic acid (DPPA), (b) salicylic acid (SA), (c) benzoic acid (BA), (d) aspirin (ASA) and (e) *p*-hydroxy benzoic acid (*p*-HOBA).

biosynthesis of prostaglandins (PGH_2) [12–14]. COX-1 synthesizes normal physiologically useful PGH_2 and COX-2 makes PGH_2 in inflammatory cells. Prostaglandins are involved in processes like pain signaling and platelet aggregations. BA is an antifungal and antibacterial drug. It is used to preserve foods and beverages. Inhibition of the growth by BA has been proposed to be due to inhibition of essential metabolic reactions [15,16]. It is also used in the treatment of skin diseases like ring worm. The compound, *p*-HOBA was used in this investigation to see how the change in the position of the functional groups attached could alter the interaction with DPPA vesicles (in SA the –OH group is *ortho* to –COOH group while in *p*-HOBA the –OH group is *para* to –COOH group).

This paper describes DSC and ^{1}H NMR studies of interaction of BA, ASA and *p*-HOBA with DPPA vesicles. The results are compared to those obtained with DPPA–SA system [11].

2. Materials and methods

2.1. Sample preparation

Lipid, L-α-DPPA, was purchased from Avanti Polar Lipids, Inc., Alabama, USA, and was used without further purification. The chemicals, acetyl salicylic acid (ASA/aspirin) and *para*-hydroxy benzoic acid (*p*-HOBA) of 99+% purities were obtained from Aldrich Chemical Company, Inc., USA. The drug, benzoic acid (99+% purity) was purchased from May and Baker, UK. The buffer of pH 9.3 was prepared using 0.2 M boric acid and 0.05 M borax ($Na_2B_4O_7{\cdot}10H_2O$) solution. The vesicles used in this investigation, were in multilamellar vesicular (MLV) and unilamellar vesicular (ULV) forms. The method of preparation of the membrane samples in the MLV and ULV forms is the same as that detailed elsewhere [11,17,18]. The weight fraction of buffer to DPPA was 2.5 in MLV. In ULV the lipid concentration [lipid], used were 50 and 25 mM for DSC and NMR experimental work, respectively. The molar ratio, R_m, of drug to DPPA was in the range, $0 \leq R_m \leq 0.5$. The ULV was prepared using buffer pH 9.3 as DPPA formed stable ULV at pH 9.3 [11,18].

For DSC measurements 7–12 mg (for MLV) and 15–18 mg (for ULV) of the samples were hermetically sealed in aluminum pans. To obtain NMR spectra, approximately 1 ml of ULV was taken in a conventional NMR tube. TLC studies on the samples were carried out to check the intactness of the lipid and drug molecules.

2.2. Differential scanning calorimeter

Perkin Elmer DSC-2C instrument was used for thermal measurements of the membrane samples, with an empty aluminum pan as a reference. The temperature and enthalpy calibrations of the DSC instrument were carried out using calorimetric standards (i) cyclohexane, with its crystal–crystal ($T_{C-C} = -89.9\,^\circ$C and $H_{C-C} = 79.6\,J\,g\,m^{-1}$) and crystal–isotropic liquid ($T_{C-I} = 6.8\,^\circ$C and $H_{C-I} = 31.3\,J\,g\,m^{-1}$) phase transitions and (ii) indium with its crystal–isotropic liquid phase transition ($T_{C-I} = 156.8\,^\circ$C and $H_{C-I} = 28.4\,J\,g\,m^{-1}$). The instrument parameters were adjusted so as to get the above values of temperature, T within $T \pm 0.5\,^\circ$C range and enthalpy, H within $H \pm 0.5\,J\,g\,m^{-1}$ range. The temperature calibration of the instrument was done, using cyclohexane and indium at a heating rate of 10 °C/min. The calibration constants required to calculate the enthalpy values, were obtained using cyclohexane, at heating rates of 10, 5 and 2.5 °C/min. The chain melting (CM) transition temperature, T_m, was obtained by extrapolating the transition peak temperatures (obtained at scanning speed of 10, 5 and 2.5 °C/min) to zero scanning speed. The area under the endothermic curve was used to obtain the transition enthalpy, ΔH_m. The scans at 5 and 2.5 °C/min were used for the calculation of CM transition enthalpies. The full width at half maximum, Δ_m, used to compare the co-operativity of the CM transitions, was obtained from 5 °C/min scans. The uncertainty in measurement of (i) enthalpy amounts to about ±2 to 10% and (ii) the T_m is about ±0.2 °C [19]. The DSC measurements were carried out for both the MLV and the ULV: (i) immediately after preparation of the respective membrane samples with equilibration time, $\tau_e \approx 0$. Experiments were repeated after equilibrating the samples at 25 °C (a) for 1 day ($\tau_e \approx 1$ day) and (b) for 30

days ($\tau_e \approx 30$ days). For each value of the molar ratio, R_m, the experiment was repeated with at least three samples. Data was considered only for those samples in which weight loss was less than 0.2 mg, at the end of the scanning experiments.

2.3. Nuclear magnetic resonance (NMR)

^{1}H NMR spectra were recorded on a Bruker Avance 500 spectrometer equipped with a calibrated temperature control at 500 MHz. ^{1}H NMR spectra were acquired using a 9000 Hz spectral width into 8 K data points, a 1 s recycle delay, an acquisition time of 0.5 s and a $\Pi/2$ pulse length of 10 μs. The number of acquisitions was 512. The water signal suppression was achieved with pre-saturation of the HDO signal during the relaxation delay of 1 s. The free induction decays (FIDs) were multiplied by a 90° phase shifted sin-bell function before Fourier transformation.

The conventional 5 mm NMR tube containing approximately 1 ml of ULV solution was used to record ^{1}H NMR spectra. D_2O was used as external reference for ^{1}H NMR experiments. The NMR spectra were recorded in the vicinity of the chain melting transition temperatures of the ULV. At each temperature the samples were equilibrated in the NMR spectrometer for at least 10 min before recording the spectra.

3. Results

The DSC heating scans of DPPA dispersion (MLV) containing increasing concentrations of BA, ASA and *p*-HOBA obtained at a scan rate of 5 °C/min, and for equilibration time, $\tau_e \approx 0$ are shown in Fig. 2a–c, respectively. The corresponding drug to lipid molar ratio (R_m)-dependence of the thermotropic parameters, the transition temperature, T_m, the transition enthalpy, ΔH_m and the transition width, Δ_m are given in Fig. 3a–c, respectively.

The DPPA ($R_m = 0$) dispersion, when heated undergoes a gel to liquid-crystalline phase transition centered at 58.3 °C and the enthalpy, ΔH_m, associated with this transition was 34.6 kJ mol^{-1} in agreement with the previous reports [20,21]. In BA, ASA and *p*-HOBA-doped DPPA dispersion, the transition temperature, T_m, increases (Fig. 3a) and the transition width, Δ_m (Fig. 3c) decreases with increasing concentration of the drug (for $R_m \leq 0.3$). However, for drug concentration, $R_m \geq 0.3$, the T_m and Δ_m values are not significantly changed (Fig. 3a). This behaviour was different from that observed with SA doped system wherein T_m value increases and Δ_m value decreases for drug concentration, $R_m \geq 0.3$ also. This is because for a given concentration of drug the interaction is least when doped with SA (Fig. 3a and b) and hence the quantity of SA required is more to get same perturbation as seen with other drugs. The presence of these drugs does not significantly change the transition enthalpy, ΔH_m of DPPA dispersion. This behaviour suggests superficial interaction between the lyophilic molecules and DPPA polar heads, which occurs only at the surface of the lipid layers.

Thermotropic parameters obtained for samples equilibrated for 1 day ($\tau_e \approx 1$ day), at 25 °C, did not change much with respect to their $\tau_e \approx 0$ values. However, equilibration for long duration ($\tau_e \approx 30$ days) at 25 °C, brings about changes in the thermotropic parameters. At any given drug concentration, the transition temperature is less than its value for $\tau_e \approx 0$ and $\tau_e \approx 1$ day, whereas the transition width is more than its value for $\tau_e \approx 0$ and $\tau_e \approx 1$ day (figures not shown). This behaviour is similar to that observed with SA [11]. Thus, prolonged equilibration results in a reduced drug–lipid interaction due to the drug molecules getting segregated out into the lipid–water interfacial region away from the lipid polar headgroup region over a period of time.

The DSC profiles, of the unilamellar vesicles (ULV) of DPPA both in the absence and the presence of the drugs BA, ASA and *p*-HOBA, obtained at the scan rate of 5 °C/min, $\tau_e \approx 0$ and for

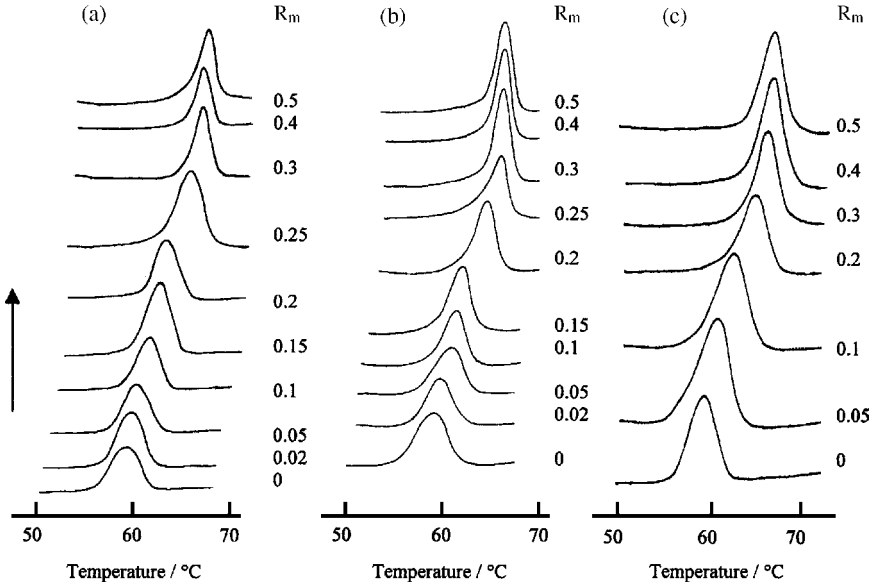

Fig. 2. The DSC heating scans at 5 °C/min of MLV containing different amount of the drugs, and for equilibration time, $\tau_e \approx 0$: (a) DPPA-BA, (b) DPPA-ASA and (c) DPPA-*p*-HOBA. The molar ratios, R_m of drug to DPPA are indicated on the curves.

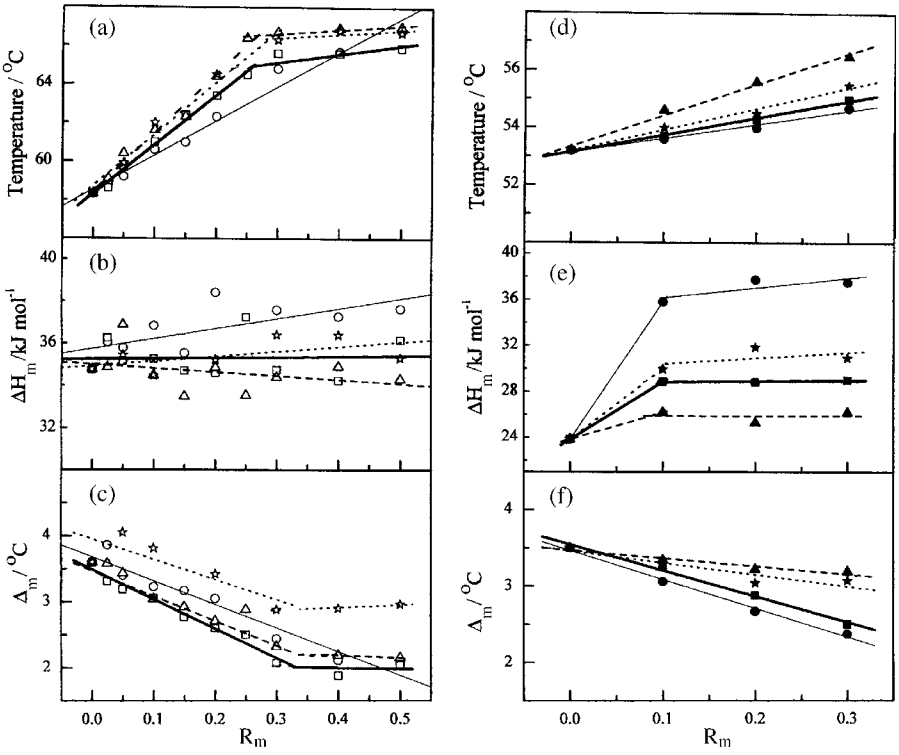

Fig. 3. R_m-dependence of transition (a and d) temperature, T_m (b and e) enthalpy, ΔH_m and (c and f) width, Δ_m for MLV [SA (◯); BA (□); ASA (△) and *p*-HOBA (☆)] and for ULV [SA (●); BA (■); ASA (▲) and *p*-HOBA (⋆)], respectively, at $\tau_e \approx 0$. The size of the symbol has been chosen in conformity with the error bar.

increasing drug concentrations, are shown in Fig. 4a–c, respectively. The R_m-dependence of the thermotropic parameters, T_m, ΔH_m and Δ_m is given in Fig. 3d–f, respectively.

The DSC heating thermograms of drug-free DPPA dispersion display an endothermic chain melting transition at a temperature 53.2 °C. The enthalpy, ΔH_m associated with this transition is 21.3 kJ mol^{-1}. However, these values are smaller than the corresponding ones for the MLV. In MLV the water molecules within the bilayers are more structured than the water molecules in ULV. Hence in MLV headgroup–headgroup interaction between the neighboring DPPA molecules is much more stronger than that in ULV. This reduced headgroup–headgroup interaction in the ULV leads to reduction in T_m value of ULV and less tight packing of the chains than in the MLV form.

In presence of the drugs, BA, ASA and *p*-HOBA, the CM transition temperature of DPPA dispersion is increased and the transition becomes sharper (Fig. 3d and f). This behaviour is similar to that observed in MLV. In contrast to the case of MLV, the CM transition enthalpy associated with the ULV increases dramatically (Fig. 3e), for $0 \leq R_m \leq 0.1$. This could probably be due to (a) increase in the size of the ULV when doped with the drug molecules and/or (b) increased rigidity of the acyl chains by the increase in the PA–PA headgroup interaction due to the presence of the drug molecules. Dynamic light scattering measurements have shown that the presence of drugs does not change the average size of the ULV significantly (in fact the size of both drug-free and drug-doped ULV is approximately 90 nm) suggesting an increase in the acyl chain order. However, with further

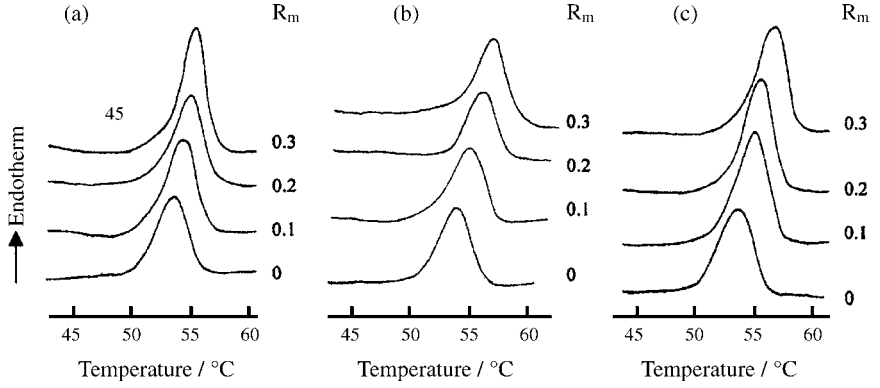

Fig. 4. DSC heating scans of ULV at 5 °C/min and for equilibration time, $\tau_e \approx 0$: (a) DPPA–BA, (b) DPPA–ASA and (c) DPPA–*p*-HOBA ([DPPA] = 50 mM). The molar ratios, R_m, of drug to DPPA, are indicated on the curves.

increase in drug concentration ($R_m > 0.1$) the ΔH_m value is not significantly changed.

Equilibration had a more pronounced effect on ULV. For example, no transition was observed for, $\tau_e \geq 1$ day for both drug-free and drug-doped membranes. It implies that equilibration destroys the ULV. Similar behaviour is observed with SA-doped DPPA dispersion [11].

^{1}H NMR experiments were carried out with drug-free, BA-doped and ASA-doped ULV of DPPA. The ^{1}H NMR spectra of DPPA obtained from (i) DPPA dispersion and (ii) BA ($R_m = 0.2$) and ASA ($R_m = 0.2$)—incorporated DPPA dispersions for various temperatures in the vicinity of T_m are shown in Fig. 5a–c, respectively. The proton resonances for the different lipidic groups can be identified with the assignments given in Fig. 1a. On comparison of drug-free and drug-doped DPPA spectra, it is seen that in both the cases the resonances, labeled 1 and 2, become sharper and better resolved as the temperature approaches T_m. The differences observed in the T_m value for ULV using NMR and DSC is due to the difference in lipid concentration (50 mM in DSC measurement and 25 mM in NMR measurement) used in these studies. At higher lipid concentration the ULV formed is either of large size or the dispersion contains vesicles with a few lamella also. Hence the T_m value of 50 mM ULV is larger than that of 25 mM ULV. With the DSC-2 Perkin Elmer instrument, 50 mM ULV had to be used due to instrument limitation. The sharpening of the chain proton resonances is indicative of greater mobility of the concerned proton due to increased chain disorder. The resonances of the various lipidic protons in the BA-doped DPPA dispersion are broader than those in the drug-free DPPA dispersion (Fig. 5a and b). This result indicates that the mobility of lipidic protons is reduced in the presence of BA, suggesting increased rigidity of the acyl chains. This behaviour is similar to that obtained for SA-doped DPPA dispersions [11]. However, ASA-doped DPPA does not show any broadening effect of the lipidic protons and the resonances were sharp even at temperature, $T < T_m$ (almost similar to that observed for $T > T_m$). Hence, in presence of ASA, the acyl chain remains disordered even for temperature, $T < T_m$. On comparing chemical shifts of drug-free and drug-doped liposomes, no significant change in the chemical shifts of the various lipidic resonances was observed with BA and ASA doped DPPA dispersion.

The ^{1}H NMR spectra of the aromatic protons from BA (labeled 11–15) and ASA (labeled 11–14) in the aqueous medium, BA-buffer/ASA-buffer at various temperatures are shown in Fig. 6a and c, respectively. The labeled BA and ASA molecules are shown in Fig. 1c and d, respectively. The spectra of the aromatic protons of BA and ASA obtained from DPPA–BA and DPPA–ASA dispersions at various temperatures around T_m are given in Fig. 6b and d. The comparison of the BA aromatic proton spectra obtained for DPPA-free (Fig. 6a) and DPPA-doped (Fig. 6b) systems indicates that the drug, BA interacts with the DPPA bilayer. The aromatic proton resonances of the BA, broadens in the presence of DPPA and the broadening increases with increasing temperature. However, the values of the chemical shift of various aromatic protons of BA are not significantly changed due to the presence of the lipid environment. The proton resonances corresponding to the –COOH group of BA is not seen due to exchange processes. Similarly on comparing the ASA aromatic proton spectra obtained for DPPA-free (Fig. 6c) and DPPA-doped (Fig. 6d) systems, it is found that there are no significant changes in the chemical shifts and the width of ASA resonances. However, additional peaks are observed (clearly seen in the DPPA-doped system) due to the hydrolysis of ASA to SA and acetic acid (Figs. 5c and 6d). The effective SA concentration was more in DPPA doped-system, as the ULV was obtained at higher temperature wherein the hydrolysis of ASA is quite high. The resonance corresponding to the methyl group in ASA occurs at 2.34 ppm and is seen as a sharp peak superimposed on the broad resonance of the lipid acyl chain proton labeled (4).

The ^{1}H NMR results suggest that the drug molecules are expected to be located near the lipid glycerol moiety and/or the polar headgroup, with its polar group interacting with (a) the vicinal water, (b) the –P=O (DPPA) group, or (c) the –C=O (DPPA) group through hydrogen bonding.

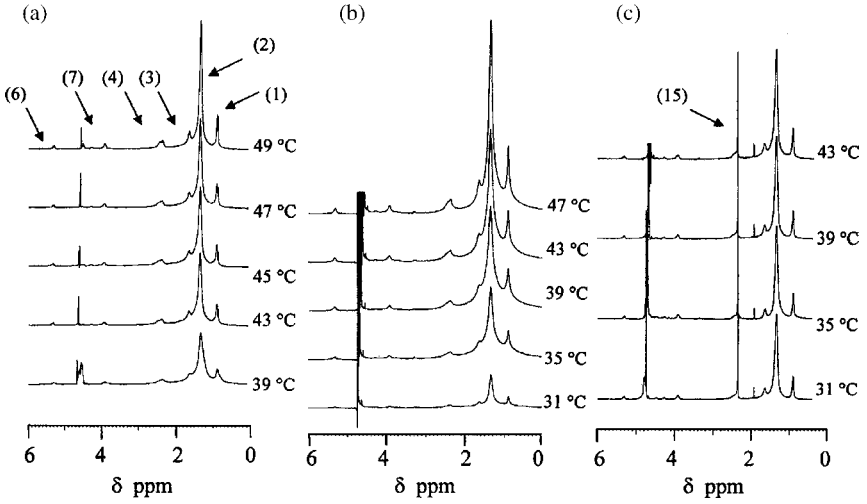

Fig. 5. ^{1}H NMR spectra of (a) DPPA ($R_m = 0$), (b) DPPA–BA ($R_m = 0.2$) and (c) DPPA–ASA ($R_m = 0.2$) in the vicinity of T_m ([DPPA] = 25 mM).

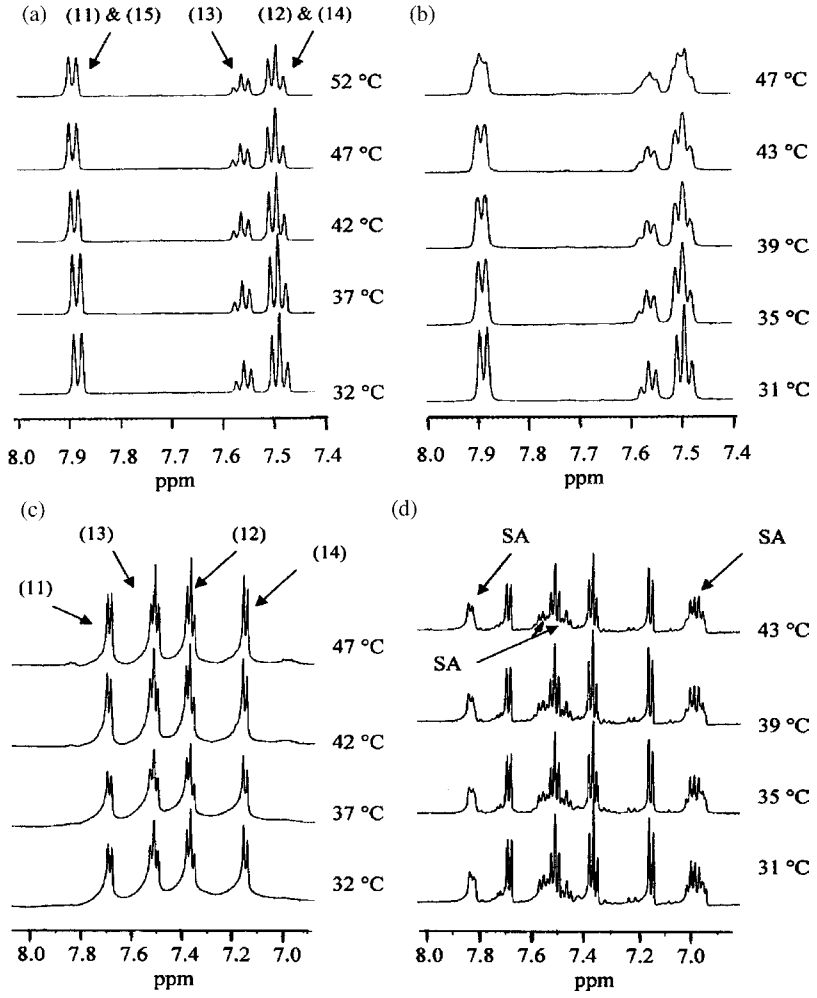

Fig. 6. Aromatic proton resonances of the drugs in (a) BA-buffer, (b) DPPA–BA-buffer ($R_m = 0.2$), (c) ASA-buffer and (d) DPPA–ASA-buffer ($R_m = 0.2$) as a function of temperature.

4. Discussion

The DSC and NMR results indicate that BA, ASA and *p*-HOBA interact with DPPA vesicles and the mode of interaction with the vesicles (both MLV and ULV) seems to be the same with all these drugs. DSC heating experiments show that the bilayer gel to liquid crystal phase transition of DPPA vesicles is influenced more by ASA, BA and *p*-HOBA than SA. The presence of BA, ASA and *p*-HOBA in DPPA dispersion increases the co-operativity between the acyl chains. The increased T_m value of the BA, ASA and *p*-HOBA-doped DPPA bilayer is indicative of the fact that the presence of these drugs increases the headgroup–headgroup interaction of the neighboring DPPA molecules. Hence, the presence of these drug reduces membrane fluidity. For a given concentration, of the drug, the rigidity of the DPPA membrane is maximum, when doped with ASA and least when doped with SA. The increase ΔT_m in the value of T_m, due to the presence of the drugs (for $R_m \leq 0.3$) can be indicated as follows: $\Delta T_{m(ASA)} > \Delta T_{m(p\text{-HOBA})} > \Delta T_{m(BA)} > \Delta T_{m(SA)}$. The acidic strength, *S*, of the –COOH group in these drugs is in the following order: $S_{SA} > S_{ASA} > S_{BA} > S_{p\text{-HOBA}}$. Hence there seems to be a good correlation between the acidity of –COOH group and the increase in T_m values (except in the case of ASA). The anomaly observed with ASA can be explained as follows: from ^{1}H NMR data, it is seen that ASA hydrolyses to SA and acetic acid (acetic acid has a pK_a value of 4.8). The increase in T_m value when the membrane is doped with ASA is higher probably due to the presence of the weak acid, acetic acid in addition to SA and ASA. Thus the reduction in the fluidity of DPPA vesicles seems to depend on the acidic strength of the –COOH group. The drugs, BA, ASA and *p*-HOBA being lyophilic in nature, it is more likely to be present in the interfacial aqueous region rather than in the acyl chain region (hydrophobic). This is supported by the observations that (a) the transition enthalpy, ΔH_m, does not change significantly, over the drug concentration range studied in MLV and (b) the presence of drugs does not change the values of the chemical shift of the various DPPA proton resonances in ULV. However, in BA, ASA and *p*-HOBA-doped ULV, the transition enthalpy increases, probably due to the enhancement in the headgroup–headgroup interaction. The broadening of the proton resonances of DPPA acyl chain in the presence of BA also indicates that the drug increases the order of the acyl chains. This behaviour was similar to that observed with SA doped DPPA system. However, in presence of ASA the

mobility of the proton resonances of DPPA acyl chains are not significantly changed. This result is in agreement with the value of the chain melting transition enthalpy obtained when doped with ASA (Fig. 3e). As seen from Fig. 3e for same drug concentration the increase in enthalpy when doped with ASA is less compared to other drugs. This could be due to the presence of acetyl group which can penetrate into co-operative region of the membrane.

According to Boggs [22] the transition temperature of PA is high over the pH range 4–10 where the state of dissociation is 0.5–1.5 and the hydrogen bond-donating and accepting groups are present. In the pH range 4–10 the transition temperature decreases with increasing pH value. The maximum in the transition temperature of PA occurs at a state of dissociation of 0.5 (at pH 4) wherein the ratio of negatively charged-to-neutral species is 1:2 and most of the negatively charged molecules will be involved in hydrogen bonding. The drop in transition temperature from pH 4 to 10 is due to the increasing concentration of negatively charged lipid as the state of dissociation increases to 1.5. This negative charge lipid will cause charge repulsion and will destabilize the gel phase lowering the transition temperature.

In buffer pH 9.3 the state of dissociation of DPPA is nearly 1.5 (i.e. the ratio of one negatively charged-to-two negatively charged species is nearly 2:1) this is supported by the obtained T_m (58.3 °C) value. The increase in transition temperature of DPPA dispersion when doped with SA, BA, ASA and *p*-HOBA suggests increased headgroup–headgroup interaction by increasing hydrogen bonding interaction. The drug molecules and DPPA molecules have been negatively charged in buffer pH 9.3 hence electrostatic interaction between them is least possible. The drug molecules seem to bring about effect similar to screening of one of the negative charge on DPPA molecules hence reducing the state of dissociation to nearly 1. This effect is supported by the observed increase in T_m value as a function of increasing drug concentration (for $R_m \leq 0.3$). However, with further increase in drug concentration ($R_m \geq 0.3$) no screening of negative charge takes place and the DPPA molecules remain with one negative charge (similar to that observed at neutral pH). Hence, for $R_m \geq 0.3$ there is no significant increase in T_m (65–66 °C) value. The transition temperature of DPPA dispersion in buffer pH 7 is reported to be 65 °C [22].

The results clearly indicate that: (i) drugs strongly interact with DPPA bilayer. (ii) The mode of interaction with the DPPA vesicles is similar in the case of all these drugs. (iii) The drug molecules are located in the aqueous interfacial region neighboring the polar groups of the phospholipids or water molecules. (iv) The drug molecules are responsible for increased PA–PA headgroup interaction. This leads to a better packing of the lipid chains and consequently, the membrane becomes more rigid (v) for a given concentration, of the drug the rigidity (r) of the DPPA membrane when doped with these drugs increase in the following order: $r_{ASA} > r_{p\text{-HOBA}} > r_{BA} > r_{SA}$. (vi) The reduction in the fluidity of DPPA membrane depends on the acidic strength of the –COOH group present in the drug molecules.

Acknowledgement

The author would like to thank Dr. P.S. Paravathanathan for fruitful discussions.

References

[1] H. Abriouel, J. Sanchez-Gonzalez, M. Maqueda, A. Galvez, E. Valdivia, M.J. Galvez-Ruiz, J. Colloid Interf. Sci. 233 (2001) 306–312.
[2] M.K. Jain, R.C. Vagner, Introduction to Biological Membranes, John Wiley, New York, 1980.
[3] M.K. Jain, Introduction to Biological Membranes, Wiley, New York, 1988.
[4] C. La Rosa, D. Grasso, M. Fresta, C. Ventura, G. Puglisi, Thermochim. Acta 195 (1992) 139–148.
[5] G.H. Lyman, D. Papahadjopoulos, H.D. Preisler, Biochim. Biophys. Acta 448 (1976) 460–473.
[6] E. Bernard, J. Francois Faucon, J. Dufourcq, Biochim. Biophys. Acta 688 (1982) 152–162.
[7] A. Bertoluzza, S. Bonora, G. Fini, O. Francioso, M.A. Morelli, Chem. Phys. Lipids 75 (1995) 137–143.
[8] T. Pott, J.-C. Maillet, C. Abad, A. Campos, J. Dufourcq, E.J. Dufourc, Chem. Phys. Lipids 109 (2001) 209–223.
[9] J. Minones Jr., J.M. Rodriguez Patino, J. Minones, P. Dynarowiczlatka, C. Carrera, J. Colloid Interf. Sci. 249 (2002) 388–397.
[10] A. Blume, J. Tuchtenhagen, Biochemistry 31 (1992) 4636–4642.
[11] L. Panicker, S.L. Narasimhan, K.P. Mishra, Thermochim. Acta 432 (2005) 41–46.
[12] D.I. DeWitt, Mol. Pharm. 55 (1999) 625–631.
[13] A.S. Kalgutkar, K.R. Kozak, B.C. Crews, G.P. Hochgesang Jr., I.J. Marnett, J. Med. Chem. 41 (1998) 4800–4818.
[14] J.R. Vane, Nature 231 (1971) 232–235.
[15] H.A. Krebs, D. Wiggins, S. Sols, F. Bedoya, Biochem. J. 214 (1983) 657–663.
[16] A.D. Warth, J. Appl. Bacteriol. 43 (1977) 215–230.
[17] L. Panicker, K.P. Mishra, J. Colloid Interf. Sci. 290 (2005) 250–258.
[18] L. Panicker, K.P. Mishra, Biophys. Chem. 120 (2005) 15–23.
[19] G.W.H. Hohne, W. Hemminger, H.-J. Flammerdheim, Differential Scanning Calorimetry: An Introduction for Practitioners, Springer, 2003.
[20] J. Minones Jr., J.M. Rodríguez Patino, J. Miñones, P. Dynarowicz-Latka, C. Carrera, J. Colloid Interf. Sci. 249 (2002) 388–397.
[21] K. Jacobson, D. Papahadjopoulos, Biochemistry 14 (1975) 152–161.
[22] J.M. Boggs, Biochim. Biophys. Acta 906 (1987) 353–404.